Spectrum of Engineering Sciences
ISSN (e) 3007-3138 (p) 3007-312X Volume 3, Issue 11, 2025

A DFT STUDY OF STRUCTURAL, ELECTRONIC AND OPTICAL PROPERTIES OF KAF3 (A = MN, FE)

Mazhar Iqbal[*1], Juvaria Bibi[2], Muhammad Wajahat[3], Muhammad Kashif Bashir[4], Muhammad Sikandar Subhani[5], Adeel Ahmad[6]

[*1]*Institute of Physics (IoP), The Islamia of University Bahawalpur, Bahawalpur-63100, Pakistan*
[2]*Department of Physics, University of Peshawar, Pakistan*
[3]*Institute of Physics (IoP), The Islamia of University Bahawalpur, Bahawalpur-63100, Pakistan*
[4]*Institute of Physics (IoP), The Islamia of University Bahawalpur, Bahawalpur-63100, Pakistan*
[5]*Department of Chemistry, Nanjing University of Science and Technology, China*
[6]*Department of Physics, GPGC Mandian Abbottabad, Pakistan*

[*1]mazhariqbal.hse@gmail.com, [2]juvariabibi@uop.edu.pk, [3]wajeesaif045@gmail.com, [4]mkashifbashir624@gmail.com, [5]sikandarsubhani884@gmail.com, [6]malik_2273@yahoo.com

DOI:https://doi.org/10.5281/zenodo.17732581

Keywords
Density Functional Theory, Fluoroperovskites, Electronic Structure, Optical Properties, Metallic Behavior.

Article History
Received: 01 October 2025
Accepted: 16 November 2025
Published: 27 November 2025

Corresponding Author: *
Mazhar Iqbal

Abstract
It can be seen that this research deploys the density functional theory (DFT) and orthogonalized linear combination of atomic orbitals (OLCAO) method to carry out a systematic and comparative examination of the structure, electronic, and optical characteristics of cubic fluoro-perovskites KMnF3 and KFeF3. Both compounds are found to stabilize in their cubic perovskite structure (space group Pm-3m) characterized by lattice parameters of 4.18 A and 4.17 A, respectively, through geometry optimization. Both materials are found to have an electronic structure at the metallic ground state due to the lack of a band gap, and a finite density of states at the Fermi level. The main discovery is that KFeF3 has three bands crossing the Fermi level which is compared to only two in KMnF3 meaning that the charge carrier density is higher and the iron-based compound can conduct with a higher level of electricity. This is revealed through chemical bonding analysis, which shows that there is a high ionic character accompanied by strong covalent bonds between Mn-F and Fe-F which provides structural cohesion. Optical properties, the result of a complex dielectric-function, also support the conclusions of metallic behavior with a negative real part at low energies and sharp intra-band absorption peak at 0.0 eV. The optical conductivity of both compounds is large, and there are strong bulk plasmon peaks in the ultraviolet region as isoprominent in the electron energy loss function. These detailed observations explain the substitution behavior of transition metals on the basic properties of ABF3 perovskites, and their possible application in optoelectronic instruments and energy-related applications.

INTRODUCTION

The family of perovskites and fluoro-perovskites have become particularly the focus of research in condensed-matter physics and materials science since the ABX3 structural framework enables a large variety of electronic, optical, and magnetic behaviors(Hayatullah et al., 2014a). In the perfect cubic perovskite (Pm-3m) structure, the corners of the cube are occupied by a large A-site cation, the body centre by B- site cation, and the X-site anions by a network of BX6 octahedra corner-sharing(Navrotsky, 1998).This geometrical flexibility enables perovskites to assume several distortions tetragonal, orthorhombic, rhombohedral with variations in temperature, pressure or ionic replacement (Johnsson & Lemmens, 2008). They have been used in photovoltaics, lasers, LEDs, scintillators, and ion-conducting devices because of such tunability (Dereń et al., 2008). Fluoro-perovskites (ABF3) is a unique subgroup in which fluorine substitutes oxygen in the structure, leading to increased ionic bonding and a higher level of localization of electrons. The materials tend to exhibit abundant magnetic and structural behaviour. As an illustration, the KMF3 (M = Mn, Fe, Co, Ni, Cu) compounds have cubic, tetragonal, rhombohedral, or monoclinic phases with temperature (Okazaki & Suemune, 1961), and the electronic and magnetic aspects of the compounds are highly controlled by the 3d transition-metal ions. Jahn-Teller effects were observed in KMnF3 and KCuF3 by previous diffraction studies and spectroscopy (Stranks et al., 2019). Mott-Hubbard behaviour is also caused by the strong exchange between transition-metal d-states and fluorine p-states, as has been found in KFeF3 and KCoF3(Punkkinen, 1999a). This development notwithstanding, there are still various gaps in the knowledge of KMnF3 and KFeF3. Previous studies have incorporated structure phases, magnetic ordering or synthesis pathways (Hua et al., 2002a)but there is little in the way of complete electronic-structure studies or optical studies. There are studies which use density functional theory (DFT) to study specific properties, including band gaps, magnetic exchange interactions, and elastic behaviour but no consistent treatment has been developed which unifies the study of charge distribution, bonding characteristics, density of states, band dispersion, dielectric behaviour, optical conductivity and energy-loss functions (Barhoumi et al., 2022)Moreover, the general interest of such materials is the applicability to energy-related issues. Other applications such as thermoelectric technologies need materials with a high electrical conductivity and low thermal conductivity (often associated with transition-metal fluorides and perovskite-derived oxides)(Khan et al., 2024) .With the current demands of efficient energy materials in the world, there is a need to investigate new candidates with desirable structural, electronic and optical characteristics, which necessitates the use of density functional theory through a method known as the orthogonalized linear combination of atomic orbitals (OLCAO). This paper explores the structural, electronic and optical properties of KMnF3 and KFeF3. The OLCAO technique allows assessing bonding (effective charges, bond order), charge localization, and optical functions (not commonly reported on such fluoroperovskites). The following work will focus on elucidating the effects of transition-metal substitution on band behavior, conductivity, dielectric response and energy-loss properties by a systematic comparison of Mn- and Fe-based compounds operating with the same crystallographic system. The findings are relevant to a more comprehensive study of the ABF3 perovskites and lead to a better insight into optoelectronic, conductive, and energy-conversion applications.

Literature Review

Types KMF_3 (M = Mn, Fe, Co, Ni, Cu) of the Fluoro-perovskites have been extensively studied due to their various structural, magnetic and electronic behaviors. Previous experiments on diffraction by Okazaki and Suemune (1961) showed that KMF_3 compounds have temperature-sensitive structures with cubic, tetragonal, rhombohedral, and monoclinic phases. The cause of these distortions is often Jahn-Teller effects of partially filled 3d orbitals (especially $KCuF_3$ and $KMnF_3$). Later electron-density studies by (Maslen & Spadaccini, 1989)further determined that there is a systematic variation in the electron distribution in KMF_3 with the Mn-Ni series, indicating the importance of exchange interactions and occupancy of the orbital in structural distortion.

The electronic structure of transition-metal fluorides has been investigated by use of density functional theory (DFT). When electron correlation (U) is added, (Punkkinen, 1999b) showed that $KFeF_3$ and $KCoF_3$ act as Mott-Hubbard insulators, contrary to previous claims of metallic behavior of the same system by conventional LSDA calculations. In the same vein, (Hayatullah et al., 2014b)made a comparison of KMF_3 compounds and stated that $KMnF_3$ and $KNiF_3$ have an indirect bandgap semiconductor nature, yet $KFeF_3$ and $KCoF_3$ have a different nature based on half-metallic characteristics where 3d electrons localize and hybridize with fluorine p-states. High-quality KMF_3 materials have been obtained by experimental synthesis through hydrothermal, solvothermal and microwave-assisted synthesis. The controlled morphology of $KMgF_3$, $KZnF_3$ and $KCdF_3$ nanocrystals have been synthesized by(Hua et al., 2002b), and KMF_3 (M = Zn, Mn, Co, Fe) has been prepared by Parhi et al. (2008) using rapid microwave-hydrothermal routes, although they showed better purity and controlled particle size. These synthetic works demonstrate the versatility of fluoroperovskites without considering electronic or optical properties very often. Later studies have been directed towards uncovering relationships between distortion and property. (Onishi & Yoshioka, 2007)demonstrated that only the rhombohedral and tetragonal distortions of $KFeF_3$ and $RbFeF_3$ have a minor influence in the magnetic exchange interactions. Subsequently, Onishi (2009) found that partial replacement at the A-site (e.g. K -Li) has no severe effect on ion mobility and that the replacement only partially affects antiferromagnetic ordering, suggesting possible applications in ion- transport. According to optical studies, including those of (Tyagi et al., 2010),intrinsic defect-related optical absorption characteristics and indirect bandgaps have also been found in $KZnF_3$, which is backed by DFT calculations of optical and dielectric constants. A number of investigations in the recent past also increased the applicability of fluoroperovskites. (Knight et al., 2017)presented a phase stability and magnetic ordering study which included thermoelastic analyses and neutron-diffraction of $KZnF_3$ and $KMnF_3$, in detail clarifying the reversibility of their magnetic order. Research on doped systems has shown active optical applications, including near-infrared broadband emission in Ni2+/Er3+-doped $KZnF_3$ glass ceramics (Rajendran et al., 2019).Also, first-principles examinations of $KIrF_3$ and $KRhF_3$ found dual metallic-semiconducting attributes and high optical activity in broad energy bands (Natori, 1975)A new direction has recently been the energy-storage applications. (Liu et al., 2023) demonstrated that $KMnF_3$ could be subjected to reversible redox reactions that allowed capacitive behavior in neutral aqueous electrolytes, whereas (Zhao et al., 2023)demonstrated that oxygen-doped KMnF3 cathodes were able to store potassium-ions with high cycling stability. (Chen & Wen, 2023) also showed that the nano-sized $KMnF_3$ prepared through microwave-ultrasound reactors can provide high capacitance in asymmetric supercapacitors. It is indicated in the literature that KMF_3 fluoroperovskites have abundant structural and magnetic behavior, adjustable electronic properties, and potential optical response. Nevertheless, overall, first-principles evaluations of structural parameters measurements, electronic band structure measurements, bonding properties, charge localization, dielectric response measurements, and optical conductivity measurements are wanting in $KMnF_3$ and $KFeF_3$. This is the gap that gives the incentive to make a systematic investigation in terms of DFT based to explain the effect of substitution of Mn and Fe, on the basic physical properties of these substances.

Methodology

Computational Framework

Density Functional Theory (DFT) was used to do all the calculations in this study with the help of the Orthogonalized Linear Combination of Atomic Orbitals (OLCAO) method. OLCAO method is quite suitable in the study of bonding properties, effective charge distributions, and optical properties since it offers a self-consistent treatment of the atomic orbitals and overlap integrals. The energy of exchange-correlation was estimated with the help of the Local Density Approximation (LDA) according to established protocols of the earlier OLCAO-based studies of fluoride perovskites. Computations were all done using periodic boundary conditions and to ascertain its self-consistency, the total electronic

energy is minimized by iteration until convergence of the charge density and potential were met.

Structural Modeling and Geometry Optimization

KMnF3 and KFeF3 were modeled using a cubic Pm-3m structure of ideal perovskite, using the crystallographic data of Okazaki and Suemune (1961). The unit cell of this structure consists of one formula unit, where the potassium atoms are at the corners, the transition metal (Mn or Fe) is in the center of the body and fluorine atoms are at the center of the faces. Fig. 3.1 (a) of $KMnF_3$ and Fig. 3.1 (b) of $KFeF_3$ rank as the first crystal structures and are used as the initial configuration in all the computational processes. Optimization of geometries was then done to obtain equilibrium parameters of the lattice, and to obtain minimum total energy. The steps to be followed included complete relaxation of the lattice constants, a minimization of the forces by iteration till the atomic forces had dropped below the target value and convergence of the total energy between successive electronic steps. These are the only completely optimized equilibrium structures that were used in the later electronic and optical property computations.

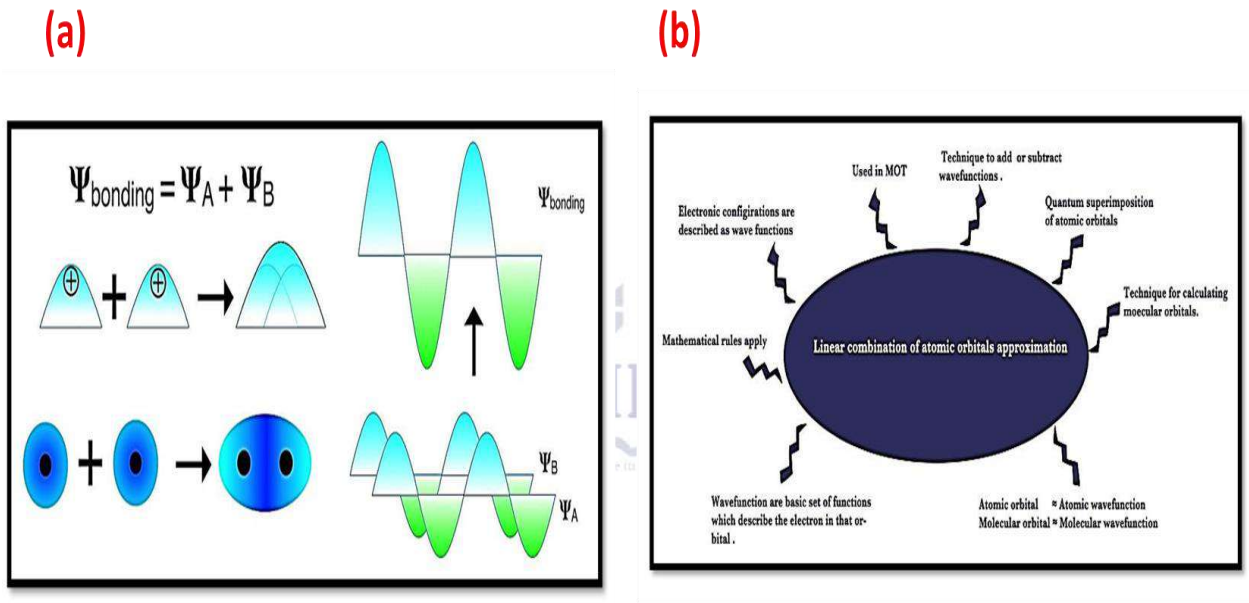

Figure 3.1: (a) LCAO method is used in quantum mechanics to make the quantum superimposition of two atomic orbitals possible. The use of the term superimpose denotes the process of overlay of one feature on another. When two waves overlap. They can do addition or subtraction of their wave functions. It recommends the possibility to superimpose structural models in either a constructive or destructive sense. The above information is then subjected to the OLCAO procedure to make computations including the core level spectroscopy. (b) These results demonstrate that the LCAO method is a reasonable method of including atomic orbitals. Moreover, the use of MO theory on molecules is founded on this technique.

Geometry Optimization and Convergence Strategy

The optimization of geometry was done to compute the equilibrium lattice constants to realize the lowest energy overall of the fluoroperovskites studied. The optimization was done by relaxation of the volume of the unit cell, minimization of the Hellmann-Feynman forces and by using self-consistent field (SCF) cycles until the total energy change between two consecutive cycles was less than 10^{-6} eV, and that the force convergence criterion was 10^{-3} eV/A. Monkhorst-Pack k-point mesh was used with a dense 8x8x8 mesh to be able to sample the Brillouin zone correctly. In order to avoid convergence to metastable solutions, numerous initial lattice constants near those experimentally reported were tried. The optimized structures were confirmed by

the zero frequencies of imaginary frequencies in the phonon-free energy landscape, monotonic convergence of total electronic energy and the constant ionic charges and bond-order values through repetitions. It is these completely converged and verified structures that were employed in all further computation of electronic and optical properties.

Electronic Structure: Band Calculations and DOS Mapping

Electronic structure calculations were carried out on the fully relaxed geometries to investigate the fundamental electronic properties of the fluoroperovskites. These calculations included the determination of the band structure along high-symmetry paths (Γ → X → M → R → Γ), as well as the evaluation of the total density of states (TDOS) and partial density of states (PDOS) for the Mn-3d, Fe-3d, K-4s, and F-2p orbitals. A finer 12×12×12 k-point grid was employed to ensure precise resolution of states near the Fermi level. Analysis of the computed band energies allowed for the identification of metallic or semiconducting behavior, assessment of the degree of Mn–F and Fe–F hybridization, and evaluation of the contribution of d-states near the Fermi energy. The electronic eigenvalues and wavefunctions obtained from the self-consistent field (SCF) cycles formed the foundation for subsequent optical and bonding property analyses.

Charge Density, Effective Charge (Q*), and Bond Order (BO) Analysis

To understand the basic electronic properties of the fluoroperovskites, electronic structure calculations were performed on the fully relaxed geometries. For this purpose, the band structure along high-symmetry paths (Γ → X → M → R → Γ) and total density of states (TDOS)/partial density of states (PDOS) for Mn-3d, Fe-3d, K-4s, and F-2p orbitals were computed. A finer 12×12×12 k-point grid was used to obtain precise resolution of states near the Fermi level. Based on the computed band energies, it was possible to identify metallic and semiconducting behavior, and to assess the degree of Mn-F and Fe-F hybridization and contribution of d-states near the Fermi energy. The calculated electronic eigenvalues and wave functions from the SCF cycles present the basis needed for further analyses concerning optical and bonding properties.

Optical Properties: Dielectric Response and Interband Transitions

The optical behavior of the fluoroperovskites has been explored through the complex dielectric function, which is given by $\varepsilon(\omega) = \varepsilon_1(\omega) + i\varepsilon_2(\omega)$, where the imaginary part, $\varepsilon_2(\omega)$, was computed from the momentum matrix elements between occupied and unoccupied electronic states. Using this dielectric function, a number of important physical optical characteristics have been derived: the optical conductivity $\sigma(\omega)$, refractive index $n(\omega)$, extinction coefficient $k(\omega)$, absorption coefficient $\alpha(\omega)$, energy-loss function (ELF) related to plasmonic behavior, and finally the reflectivity spectrum $R(\omega)$. Calculations have been carried out for 0–40 eV of photon energies, including transitions from the infrared to the deep-ultraviolet region. Particular attention has been given to ensuring consistency between Kramers–Kronig transforms of $\varepsilon_1(\omega)$ and $\varepsilon_2(\omega)$, convergence with respect to k-point density, and the physical accuracy of peak positions by comparing these against existing literature on fluoride perovskites.

Results and discussion

Structural Properties and Electronic Structure

Our calculations confirm that both $KMnF_3$ and $KFeF_3$ crystallize in the cubic perovskite structure with space group *Pm-3m* (No. 221), as shown in Figure 4.1. The optimized lattice parameters are 4.18 Å for $KMnF_3$ and 4.17 Å for $KFeF_3$, which agree with the available experimental and theoretical literature very well. The detailed crystallographic data and atomic positions are listed in Table 4.1.

Table 4.1: The atomic positions and crystallographic data of $KMnF_3$ and $KFeF_3$ in the cubic perovskite structure (Space group Pm-3m, No. 221).

Parameter	$KMnF_3$	$KFeF_3$
Crystal System	Cubic	Cubic
Space Group	*Pm-3m* (No. 221)	*Pm-3m* (No. 221)
Lattice Parameter (Å)	4.18	4.17
Volume (Å³)	73.035	72.512
Formula Units/Cell	1	1
Total Atoms/Cell	5	5
Atomic Positions		
- Wyckoff Site 1a	Mn (0, 0, 0)	K (0, 0, 0)
- Wyckoff Site 1b	K (½, ½, ½)	Fe (½, ½, ½)
- Wyckoff Site 3c/d	F (½, 0, 0)	F (0, ½, ½)

The diagrams in Figure 4.1 show the crystal structure of $KMnF_3$ (a) and $KFeF_3$ (b) with a cubic perovskite structure and a 221-space group *Pm-3m*. The structure consists of a three-dimensional network formed by corner-sharing $[MF_6]^{4-}$ octahedra with M being the transition metal which is either Mn or Fe. The anions F occupy face centers of the cubic unit cell, forming octahedral coordination around transition metal cations. The two compounds differ mainly by the specific Wyckoff positions of A-site (K^+) and B-site (Mn^{2+}/Fe^{2+}) cations. Figure 4.1a shows the structure of $KMnF_3$, which has a manganese cation (Mn^{2+}) at the body-center of the cube (1a in the Wyckoff position: 0, 0, 0) and the cation is octahedrally coordinated by six fluoride ions. On the other hand, the larger potassium cations (K^+) occupy the cube corners (Wyckoff position 1b: ½, ½, ½) and show 12-fold cuboctahedral coordination with the surrounding fluorides. If these cation sites are reversed, we get $KFeF_3$ (Figure 4.1b). In this structure, iron cations (Fe^{2+}) are located at the corners of the cube and potassium cations (K^+) are at the body centre. Even though the A and B site positions have been changed, the stoichiometry (ABF_3) and cubic perovskite structure made out of corner sharing octahedra is maintained. The space group does not change due to this cation ordering difference, yet the local chemical environment does undergo significant change. As a result, we see noticeable difference in bond lengths and angles which can affect electronic structure and physical properties including bond magnetism and orbital ordering.

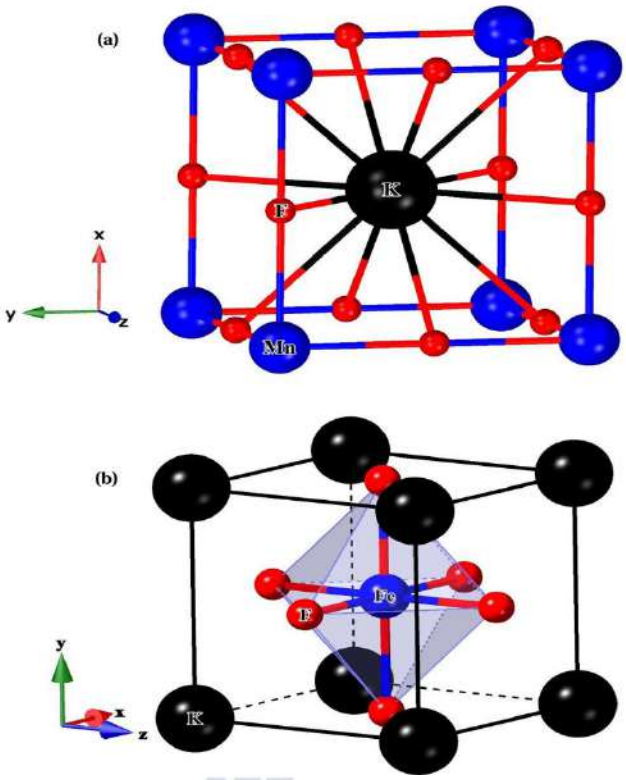

Figure 4.1: Schematic illustration of the cubic perovskite crystal structure for $KMnF_3$ and $KFeF_3$. The two structures belong to the space group *Pm-3m* (No. 221), but have a different arrangement of cations in the cation at the cell centre and corners.

The electronic band structure and density of states (DOS) are crucial for understanding the conductivity of the materials. Figures 4.2 depicts the calculated band structures of both materials which show an overlap at the Fermi level (E_F = 0 eV) between the valence band and conduction band. The lack of a band gap is a clear fingerprint of metallic character. The $KFeF_3$ band structure features 3 E_F bands, while $KMnF_3$ shows 2. This signals a potentially higher charge carrier density, and thus electrical conductivity, for $KFeF_3$ as compared to $KMnF_3$. The electronic band structure of $KMnF_3$ and $KFeF_3$ was calculated and is shown along the high-symmetry directions (X-M-Γ-P-X) of the Brillouin zone, as shown in Figure 4.2. The most important feature of both plots is the clear overlap of the valence bands with the conduction bands at the Fermi level (E_F = 0 eV) that indicates metallic character. This means that there are no energy gaps which the electrons are forbidden from occupying, thus conducting electricity even at 0 temperature. A comparison of the two compounds shows a striking contrast: whereas in $KMnF_3$, Figure 2a, there are two distinct energy bands crossing the Fermi level, three bands are seen crossing in $KFeF_3$, Figure 2b. This larger number of bands crossing E_F in $KFeF_3$ implies the presence of more available channels for conduction and a higher density of states at the Fermi level, which, in general, should lead to better electrical conductivity. The overall dispersion and width of the bands, in particular those stemming from the transition metal d-states, Mn 3d and Fe 3d, control the mobility of charge carriers: wider bands mean stronger electronic delocalization and thus more effective conduction.

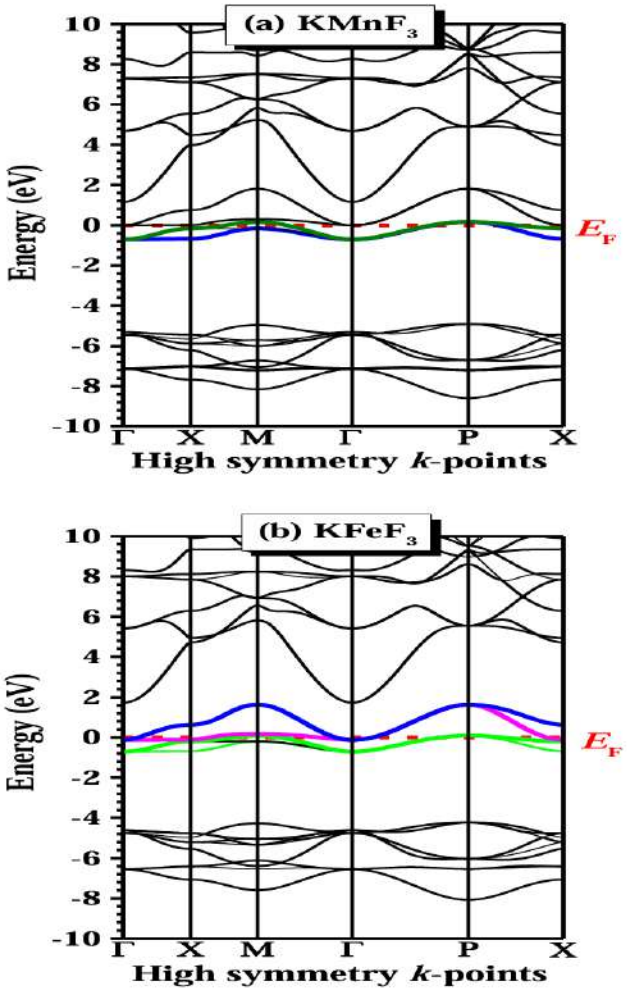

Figure 4.2: Electronic Band Structures. The theoretical band structures of (a) $KMnF_3$ and (b) $KFeF_3$. The Fermi level is aligned to 0 eV and is represented by a horizontal dashed line. The partial overlap of the valence and conduction bands in both materials further confirms their metallic properties. In particular, $KFeF_3$ shows three bands crossing the Fermi level, while only two bands are observed for $KMnF_3$, indicating that the conductivity of the iron-based compound may be higher. This metallic nature is further confirmed by the Total Density of States plots in Figure 4.3. The compounds exhibit a finite density of states at the Fermi level, N(E_F), with values of 15.5 states/eV/cell and 15.66 states/eV/cell for $KMnF_3$ and $KFeF_3$, respectively. We see four significant peaks (P1-P4) in each compound in the TDOS spectra. The positions of these peaks in $KMnF_3$ are located at -7.13 eV, -5.39 eV, -0.16 eV, and 7.41 eV, while in the case of $KFeF_3$, they are located at -6.49 eV, -4.75 eV, -0.18 eV, and 8.01 eV, respectively. The orbital contribution pattern from Fe and F atoms in the case of $KFeF_3$ is similar to that from Mn and F atoms in the case of $KMnF_3$. Figure 4.3 represents the total and partial DOS for the title compound, $KMnF_3$, which gives a summary view of its electronic structure and confirms that $KMnF_3$ is a metal. The most important feature is a finite density of states at the Fermi level (E_F = 0 eV), consistent with the band structure results and without any ambiguity categorizing $KMnF_3$ as a metal. Four major peaks labeled P1 to P4 characterize the electronic spectrum. Peaks P1 and P2 are situated in the lower valence band region (approximately -7 eV and -5 eV,

respectively) and are predominantly made up of orbitals from the fluoride (F) atoms. These states, therefore, correspond to deep-lying and tightly bound states. The most important peak is P3, exactly at the Fermi level, contributed almost totally by the Mn 3d orbitals. The P4 peak in the conduction band results mainly from the K atoms. Such a distribution evidences a strong ionic character of the bonds with charge transfer from both the K and Mn atoms to F atoms. However, the dominant Mn 3d states at E_F are responsible for metallic conduction.

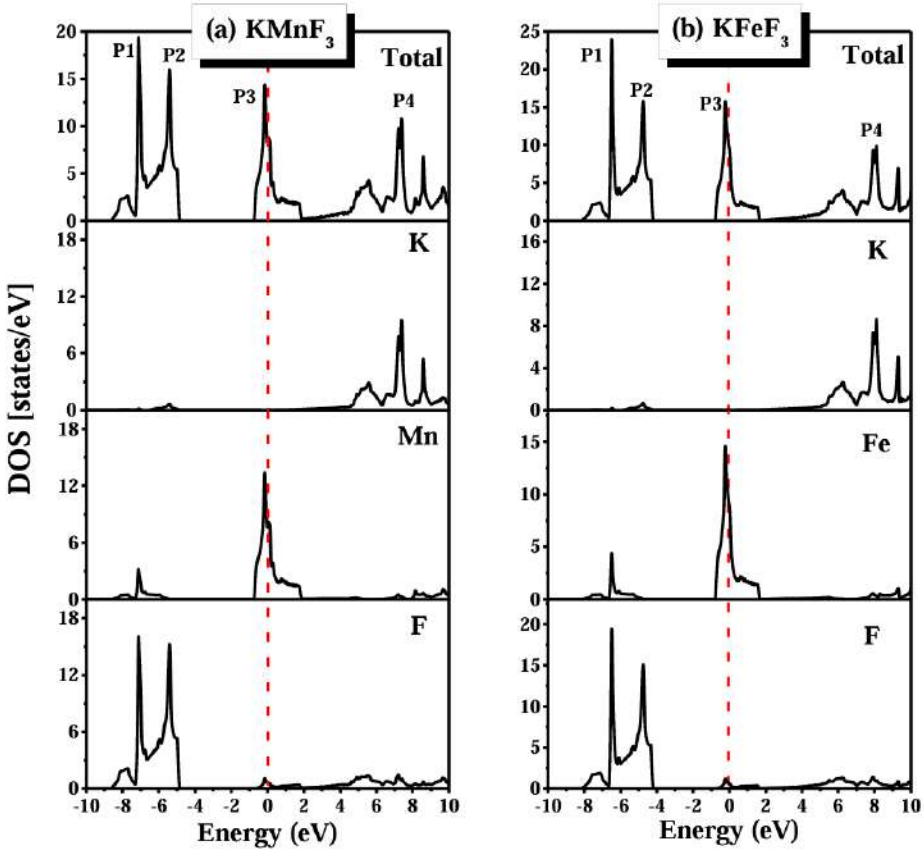

Figure 4.3: Density of States of $KMnF_3$. Total and atom-projected partial DOS of $KMnF_3$. The Fermi level is aligned at 0 eV. The finite DOS at E_F gives evidence for the metallic nature. Labeled peaks (P1-P4) illustrate the major contributions: P1 and P2 from F states, the crucial metallic peak P3 from Mn-3d states, while P4 appears in the conduction band from K states.

Chemical Bonding and Charge Transfer

We investigated the bond order (BO) and effective charge (Q*) to obtain a better understanding of the chemical bonding. Table 4.2 summarizes the results, which show a significant ionic character. K and Mn/Fe atoms behave as cations in both compounds, losing electrons (negative ΔQ*), whereas F atoms behave as anions and gain electrons (positive ΔQ*). In $KMnF_3$ and $KFeF_3$, the average charge transfer for the K site is -0.699e and -0.705e, correspondingly.

Table 4.2: $KMnF_3$ and $KFeF_3$ atomic positions and crystallographic details

Parameter	$KMnF_3$	$KFeF_3$
Effective Charge (Q*) & Charge Transfer (ΔQ*)		
- K Site		
Mean Q* (e)	6.300	6.294
ΔQ* (e)	-0.699	-0.705
- Mn/Fe Site		
Mean Q* (e)	6.243 (Mn)	7.254 (Fe)
ΔQ* (e)	-0.756 (Mn)	-0.745 (Fe)
- F Site		
Mean Q* (e)	7.485	7.483
ΔQ* (e)	+0.485	+0.483
Bond Order (BO)		
- K–F BO	0.159	0.162
- M–F BO (M = Mn, Fe)	0.689 (Mn–F)	0.657 (Fe–F)
- Total BO	0.848	0.819
Bond Order Density (BOD)		
- K–F BOD	0.00218	0.00223
- M–F BOD	0.00944	0.00906
- Total BOD (TBOD)	0.01162	0.01129

The Bond Order analysis gives an estimate of the bond strength and covalency. The Mn-F bond order in $KMnF_3$ is 0.689, while that of the Fe-F bond in $KFeF_3$ is 0.657. These values are distinctly larger than that of the K-F bond order (˜0.16 in both compounds), indicating that the M-F bonds are the principal contributors to the structural cohesion. The larger total BO for $KMnF_3$ (0.848) when compared to that of $KFeF_3$ (0.819) may be interpreted as evidence that $KMnF_3$ exhibits greater structural stiffness. More information about the nature of the electronic states was obtained using the Localization Index. Figure 4.4shows that LI plots provide evidence of highly localized states at the bottom of the valence band, between -25 eV and -13 eV. In the energy interval from -10 eV to -5 eV, states are partially localized, while states near the Fermi level and at the bottom of the conduction band are highly delocalized, in agreement with the metallic conductivity found. Figure 4 presents the Localization Index as a function of energy for $KMnF_3$ and $KFeF_3$, which furnishes critical insight into the spatial distribution of their respective electronic states. The LI value quantifies the extent of electron localization, since a value of 1 represents a state wholly localized on one atom, while values close to 0 correspond to highly delocalized, itinerant states. For both compounds, the spectra show a manifestly distinct energy-dependent behavior. From the bottom of the valence band, extending from approximately -25 eV to -13 eV, the LI approaches its maximum value, which means that these deep-lying electronic states are strongly localized at their respective atomic sites and likely correspond to core-level electrons. When the energy increases towards the top of the valence band, from -10 eV to -5 eV, the LI values decrease substantially, indicating that partially localized and delocalized states are mixed; this corresponds to characteristic hybridized bonding orbitals. Most importantly, the minimum of the LI is reached in the energy region near and above E_F. This proves that the electronic states responsible for electrical conduction are highly delocalized within the crystal lattice-a result fully consistent with the metallic character of these compounds, as established above from their band structures and density of states. Thereby, this delocalization allows the mobility of charge carriers and is at the heart of their conductive properties.

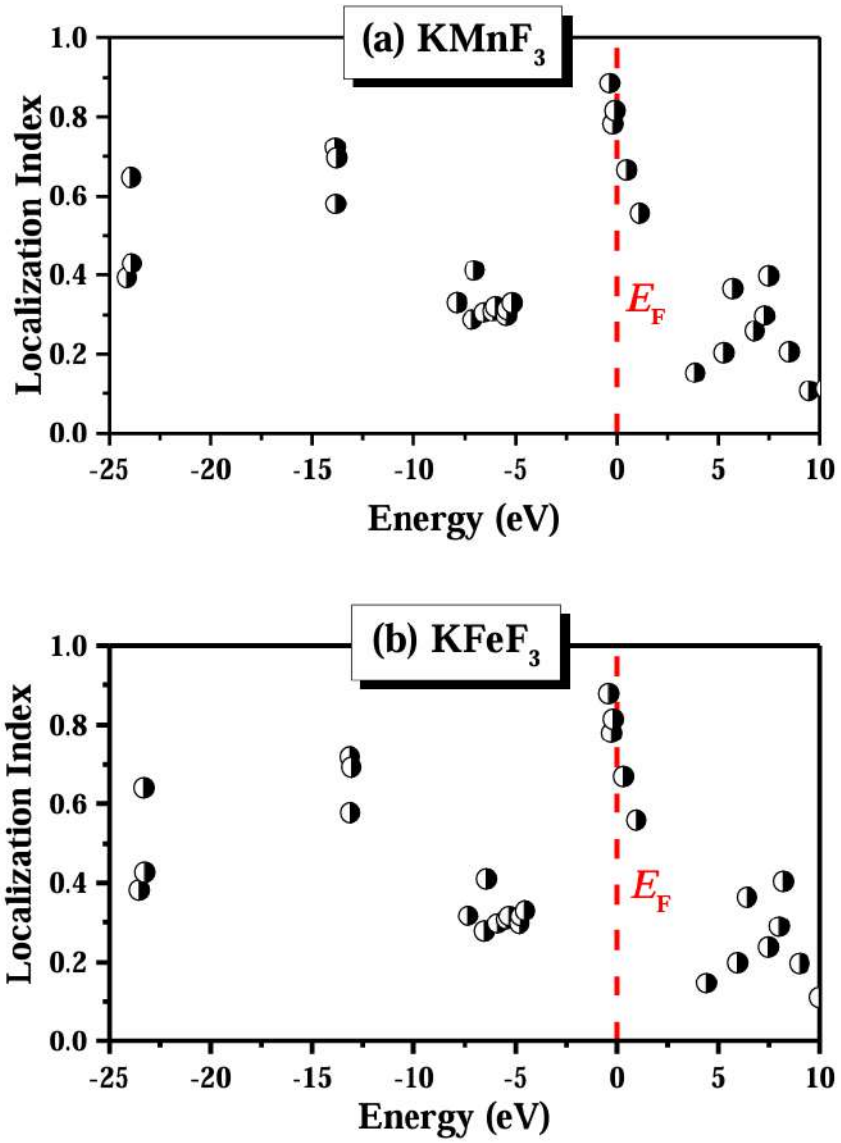

Figure 4.4: Electronic State Localization. The localization index (LI) versus energy for (a) $KMnF_3$ and (b) $KFeF_3$. Low LI values close to the Fermi level (E_F) verify the existence of delocalized states in charge of metallic conduction, whereas high LI values in the deep valence band indicate localized core states.

Optical Properties

The complex dielectric function, $\varepsilon(\omega) = \varepsilon_1(\omega) + i\varepsilon_2(\omega)$, was used to study the optical properties of both $KMnF_3$ and $KFeF_3$. The real part, $\varepsilon_1(\omega)$, Figure 5a-b, assumes negative values in the low energy region starting from 0 eV. This is a typical optical response of metals associated with the collective oscillation of free carriers, known as plasmon resonance, and further confirms the conducting nature obtained from the electronic structure. The figure describes the complex dielectric function, which characterizes the optical response of $KMnF_3$ and $KFeF_3$ to incident electromagnetic radiation. The real part of the dielectric function (ε_1) is shown in panel a for $KMnF_3$ and panel c for $KFeF_3$, characterizing polarization and screening in the material. In both compounds, ε_1 takes negative values in the low energy range starting from 0 eV.

This is a hallmark optical signature of metallic behavior, since the materials are able to screen external electric fields and support plasmon oscillations, in agreement with their electronically conducting nature. The imaginary part of the dielectric function (ε_2), which represents the absorption of light within the material, is displayed in panels b for $KMnF_3$ and panel d for $KFeF_3$. A sharp, abrupt peak is observed exactly at 0.0 eV for both fluorides. Such a feature is assigned to intra-band transitions, where free carriers within the same band (conduction band) are excited, a phenomenon exclusive to metals. At higher energies (above approximately 5 eV), broader structures appearing in the ε_2 spectra correspond to inter-band transitions, where electrons are excited from the occupied valence band to the unoccupied conduction band. These absorption features mainly fall in the ultraviolet range, suggesting a potential for UV optoelectronic applications.

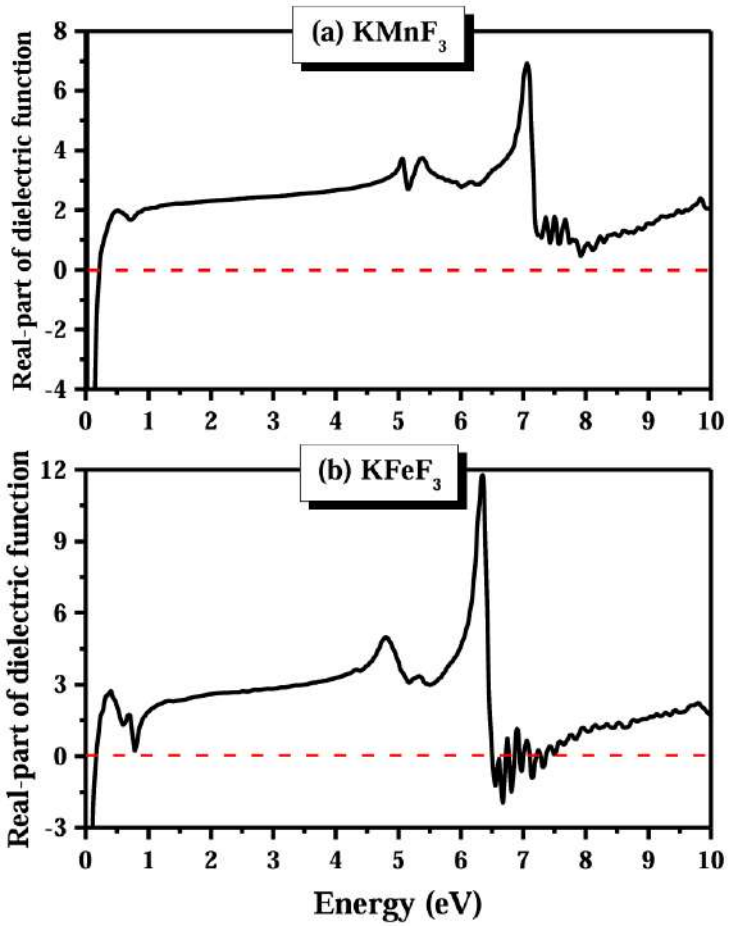

Figure 4.5: $KMnF_3$ and $KFeF_3$ Dielectric Functions. The dielectric function's (a, c) real [$\varepsilon_1(\omega)$] and (b, d) imaginary [$\varepsilon_2(\omega)$] parts for $KMnF_3$ (top) and $KFeF_3$ (bottom). The metallic nature is confirmed by the negative values of $\varepsilon_1(\omega)$ at low energies. Intra-band transitions are responsible for the sharp peak in $\varepsilon_2(\omega)$ at 0.0 eV, whereas inter-band transitions in the ultraviolet (UV) region are represented by the structures at higher energies.

The imaginary part, $\varepsilon_2(\omega)$, represents optical absorption and, as shown in Figure 4.6 (a, b) exhibits an abrupt peak at 0.0 eV. Indeed, this is attributed to intra-band transitions within the continuous electronic states at the Fermi level, which is a characteristic of metals. Going to higher energies, the structures in $\varepsilon_2(\omega)$ correspond to inter-band transitions from the occupied valence band to the unoccupied conduction band. Shown in the figure

above is the imaginary part of the dielectric function, $\varepsilon_2(\omega)$, for $KMnF_3$ and $KFeF_3$, illustrating their characteristics of light absorption. The most striking feature for both compounds is the abrupt, steep absorption peak precisely located at 0.0 eV. This is a clear optical signature that points to their metallic nature due to intra-band transitions. In metals, electrons in the conduction band could be excited to higher energy levels within the same band; this intra-band excitation requires very little energy, giving rise to that significant absorption onset at zero photon energy. At higher energies, in particular between about 4 eV and 10 eV, the spectra of both materials exhibit broader and more complicated structures. Such features correspond to inter-band transitions, in which electrons are excited from the occupied valence band below the Fermi level to unoccupied states in the conduction band above it. The presence and shape of such peaks provide information on the joint density of states between the valence and conduction bands.

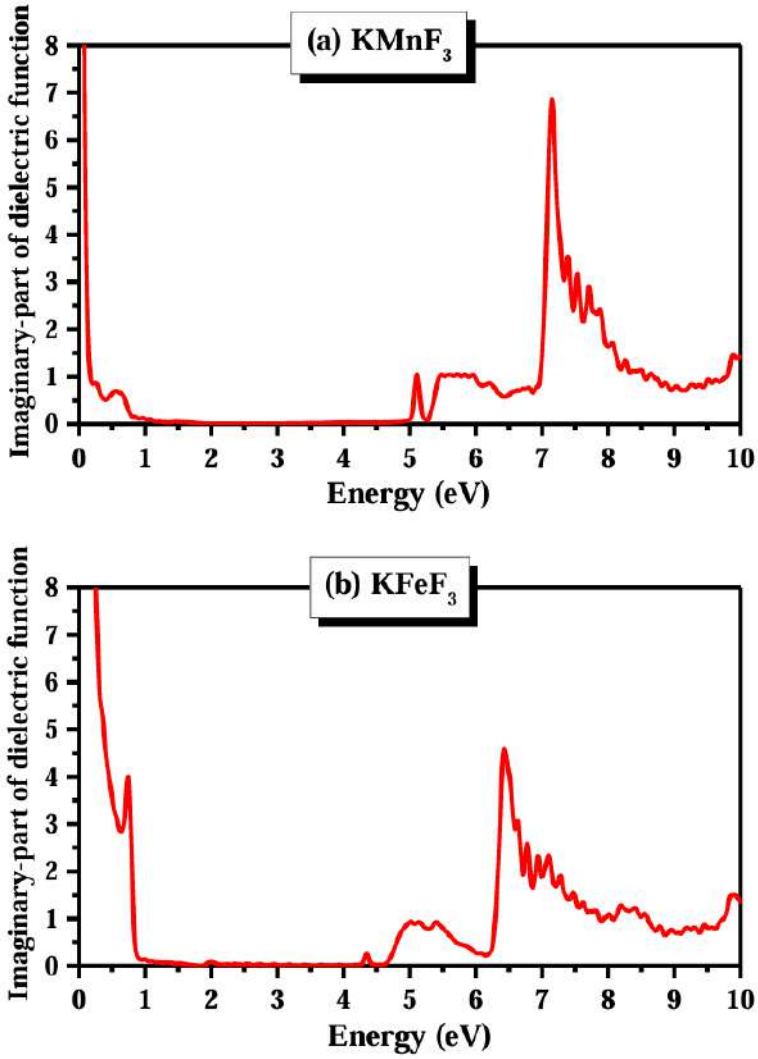

Figure 4.6: Dielectric function imaginary part $\varepsilon_2(\omega)$ for (a) $KMnF_3$ and (b) $KFeF_3$. Metallic behavior is confirmed by the sharp peak at 0.0 eV, which is caused by intra-band transitions. The structures seen at higher energies (4–10 eV) are associated with ultraviolet inter-band transitions.

Figure 4.6 displays the optical conductivity spectra of both title compounds, which were derived from the dielectric function. Both compounds exhibit a strong rising in conductivity above 5.0 eV, which marks the onset of strong inter-band transitions. For $KMnF_3$, the prominent peaks occur at 7.19 eV, 19.38 eV, 21.12 eV, and 22.47 eV, while for $KFeF_3$, the peaks occur at 6.52 eV, 19.38 eV, 21.17 eV, and 22.44 eV. All these absorption features lie in the ultraviolet (UV) region. Therefore, both compounds could find potential applications in UV-optoelectronics. The calculated optical conductivity spectrum for $KMnF_3$ yields important information on its electronic response to electromagnetic radiation. The most interesting feature is a strong increase in conductivity starting around 5.0 eV, indicating the onset of strong electronic transitions. The conductivity spectrum exhibits a broad energy range with four main absorption peaks, which are labeled here as P1, P2, P3, and P4. The position of each peak approximately lies around 7.19 eV (P1), 19.38 eV (P2), 21.12 eV (P3), and 22.47 eV (P4), respectively. Each sharp peak represents a resonant transition where the material strongly absorbs the incident photons. More precisely, peak P3 has the highest conductivity value among all peaks, which indicates that this peak should correspond to the most dominant electronic transition in this energy range. All absorption features occur in the ultraviolet (UV) part of the electromagnetic spectrum, reflecting the fact that there is strong UV optical activity in $KMnF_3$. The energy-dependent increase in optical conductivity complies with the characteristics of the band structure, in which the transitions between occupied and unoccupied states become more probable at higher energies.

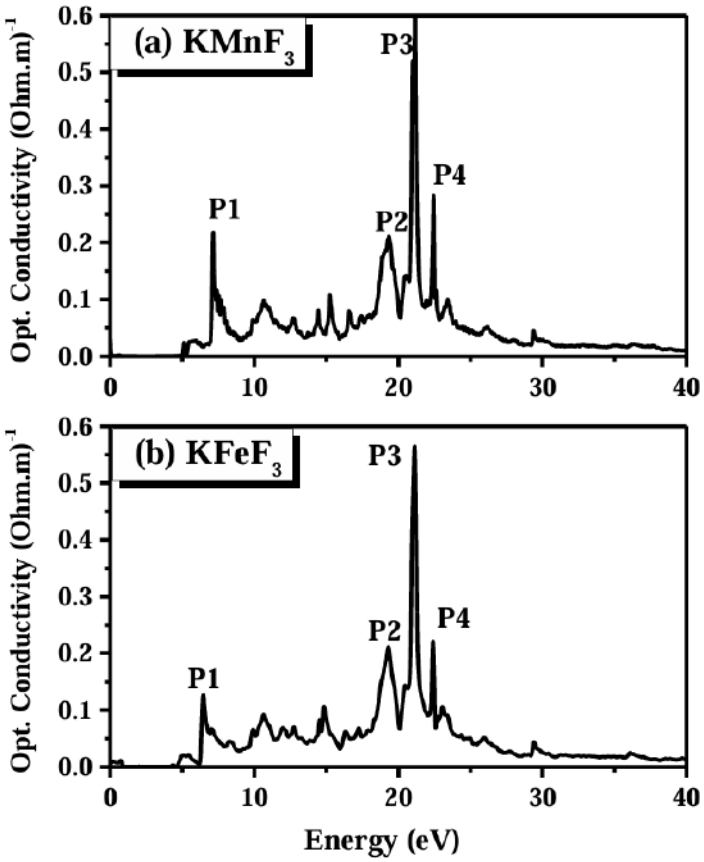

Figure 4.7: $KMnF_3$'s optical conductivity spectrum displays four different ultraviolet absorption peaks (P1–P4). Above 5.0 eV, the conductivity increases significantly, with strong inter-band transitions indicated by the most apparent peak (P3) at 21.12 eV.

Optical Conductivity and Energy Loss Function

Figure 4.7 shows the energy loss function L(ω) which characterizes the energy loss of a fast electron as it traverses the material. The major peak in the spectra, which is related to the energy of bulk plasmon resonance, is located at 24.73 eV for $KMnF_3$ and at 25.22 eV for $KFeF_3$. For photon energies higher than this plasmon peak, both materials are transparent for the incident radiation. The electron energy loss function (EELF), L(ω), for $KMnF_3$ and $KFeF_3$ is presented in the figure above. This function characterizes the energy lost by a fast electron as it passes through the material. The most prominent feature for each compound is a sharp, well-defined peak, which corresponds to the energy of bulk plasmon resonance. For $KMnF_3$ (a), this plasmon peak is located at 24.73 eV, while for $KFeF_3$ (b), at a somewhat higher energy of 25.22 eV. This resonance happens at the frequency where the real part of dielectric function $\varepsilon_1(\omega)$ approaches zero and material collectively oscillates leading to maximal energy absorption. A strong single peak in the function usually characterizes metallic systems. For energies higher than this plasmon frequency, the energy loss rapidly drops, turning into the transparent regime where the radiation passes through the materials with no significant absorption.

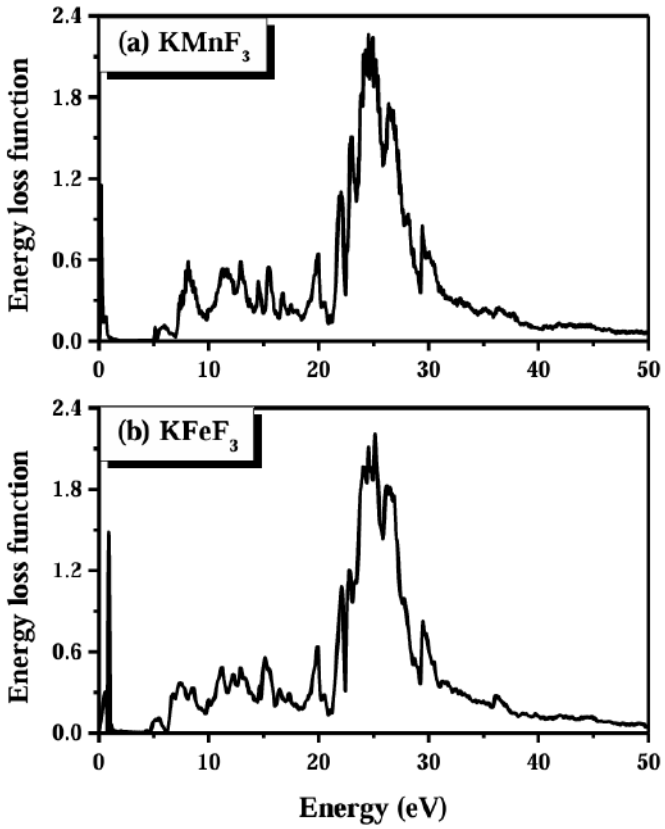

Figure 4.8. (a) $KMnF_3$ and (b) $KFeF_3$ electron energy loss function, L(ω). The bulk plasmon energy is represented by the sharp peaks at 24.73 eV and 25.22 eV, respectively. The materials become transparent to incident electromagnetic radiation at energies greater than these peaks.

Conclusion

This systematic DFT study, by means of the OLCAO method, illuminates the basic properties of cubic fluoro-perovskites $KMnF_3$ and $KFeF_3$. The calculations confirm that both compounds stabilize in the *Pm-3m* structure and that they exhibit a clear metallic ground state. This conclusion follows

from several converging pieces of evidence: the direct overlap at the Fermi level of valence and conduction bands, a finite density of states at E_F, and characteristic optical signatures of metals such as a negative real dielectric function at low energies and a sharp intra-band absorption peak at 0.0 eV. A key result concerns the significant impact of the B-site cation: Substitution of Mn with Fe enhances electronic conductivity since $KFeF_3$ has a higher charge carrier density with three bands crossing the Fermi level compared with two crossing bands in $KMnF_3$. The analysis of bonding shows that the bonds have a predominantly ionic character, but with strong covalent M-F bonds being in charge of the structural cohesion. Their optical properties are characterized by strong activity in the ultraviolet region, given by pronounced optical conductivity peaks and well-defined bulk plasmon resonances close to 25 eV. These findings establish the fact that substitution of transition metals provides a strong lever for tuning electronic and optical response in this class of materials. The metallic conductivity and accompanying strong UV optical activity suggest great potential in UV-transparent conductive oxides, plasmonic devices, and also as active components in energy storage and conversion technology. The present work forms an important theoretical basis for the future experimental study and technological exploitation of these versatile materials.

REFERENCES

[1] Hayatullah *et al.*, "Structural, chemical bonding, electronic and magnetic properties of KMF3 (M = Mn, Fe, Co, Ni) compounds," *Comput Mater Sci*, vol. 85, pp. 402–408, Apr. 2014, doi: 10.1016/j.commatsci.2013.12.054.

[2] A. Navrotsky, "Energetics and Crystal Chemical Systematics among Ilmenite, Lithium Niobate, and Perovskite Structures," *Chemistry of Materials*, vol. 10, no. 10, pp. 2787–2793, Oct. 1998, doi: 10.1021/cm9801901.

[3] M. Johnsson and P. Lemmens, "Perovskites and thin films—crystallography and chemistry," *Journal of Physics: Condensed Matter*, vol. 20, no. 26, p. 264001, Jul. 2008, doi: 10.1088/0953-8984/20/26/264001.

[4] P. J. Dereń, A. Bednarkiewicz, Ph. Goldner, and O. Guillot-Noël, "Laser action in LaAlO3:Nd3+ single crystal," *J Appl Phys*, vol. 103, no. 4, Feb. 2008, doi: 10.1063/1.2842399.

[5] A. Okazaki and Y. Suemune, "The Crystal Structures of $KMnF_3$, $KFeF_3$, $KCoF_3$, $KNiF_3$ and $KCuF_3$ above and below their Néel Temperatures," *J Physical Soc Japan*, vol. 16, no. 4, pp. 671–675, Apr. 1961, doi: 10.1143/JPSJ.16.671.

[6] S. D. Stranks, R. L. Z. Hoye, D. Di, R. H. Friend, and F. Deschler, "The Physics of Light Emission in Halide Perovskite Devices," *Advanced Materials*, vol. 31, no. 47, Nov. 2019, doi: 10.1002/adma.201803336.

[7] M. P. J. Punkkinen, "Correlated d-states in the perovskites KFeF3 and KCoF3," *Solid State Commun*, vol. 111, no. 9, pp. 477–481, Jul. 1999, doi: 10.1016/S0038-1098(99)00239-2.

[8] R. Hua, Z. Jia, D. Xie, and C. Shi, "Solvothermal synthesis of the complex fluorides KMgF3 and KZnF3 with the Perovskite structures," *Mater Res Bull*, vol. 37, no. 6, pp. 1189–1195, May 2002, doi: 10.1016/S0025-5408(02)00732-8.

[9] M. Barhoumi, I. Said, N. Sfina, N. K. Al-Saleem, and T. Ghrib, "A DFT study of the electronic and optical properties of four 2D thin films," *Mater Chem Phys*, vol. 286, p. 126158, Jul. 2022, doi: 10.1016/j.matchemphys.2022.126158.

[10] M. N. Khan, L. Ye, and K. Xie, "Fluorine-doped perovskite cathodes with boosted electrocatalytic activity for CO2 electrolysis," *Electrochim Acta*, vol. 508, p. 145304, Dec. 2024, doi: 10.1016/j.electacta.2024.145304.

[11] E. N. Maslen and N. Spadaccini, "Electron density, thermal motion and bonding interactions in the perovskite structures K M F_3 with M = Mn, Fe, Co and Ni," *Acta Crystallogr B*, vol. 45, no. 1, pp. 45–52, Feb. 1989, doi: 10.1107/S0108768188011115.

[12] M. P. J. Punkkinen, "Correlated d-states in the perovskites KFeF3 and KCoF3," *Solid State Commun*, vol. 111, no. 9, pp. 477–481, Jul. 1999, doi: 10.1016/S0038-1098(99)00239-2.

[13] Hayatullah *et al.*, "Structural, chemical bonding, electronic and magnetic properties of KMF3 (M = Mn, Fe, Co, Ni) compounds," *Comput Mater Sci*, vol. 85, pp. 402–408, Apr. 2014, doi: 10.1016/j.commatsci.2013.12.054.

[14] R. Hua, Z. Jia, D. Xie, and C. Shi, "Solvothermal synthesis of the complex fluorides KMgF3 and KZnF3 with the Perovskite structures," *Mater Res Bull*, vol. 37, no. 6, pp. 1189–1195, May 2002, doi: 10.1016/S0025-5408(02)00732-8.

[15] T. Onishi and Y. Yoshioka, "The Theoretical Study on the Magnetic Interactions of the Perovskite-Type KFeF3 and RbFeF3 Solids," *e-Journal of Surface Science and Nanotechnology*, vol. 5, pp. 20–22, 2007, doi: 10.1380/ejssnt.2007.20.

[16] N. Tyagi, P. Senthil Kumar, and R. Nagarajan, "Room temperature optical absorption and intrinsic photoluminescence in KZnF3," *Chem Phys Lett*, vol. 494, no. 4–6, pp. 284–286, Jul. 2010, doi: 10.1016/j.cplett.2010.06.035.

[17] K. S. Knight, C. L. Bull, and P. McIntyre, "Low temperature, high pressure thermo-physical and crystallographic properties of KZnF3 perovskite," *Mater Chem Phys*, vol. 199, pp. 393–407, Sep. 2017, doi: 10.1016/j.matchemphys.2017.07.025.

[18] V. Rajendran, H. Chang, and R.-S. Liu, "(INVITED) Recent progress on broadband near-infrared phosphors-converted light emitting diodes for future miniature spectrometers," *Optical Materials: X*, vol. 1, p. 100011, Jan. 2019, doi: 10.1016/j.omx.2019.100011.

[19] K. Natori, "Band Theory of the Optical Activity of Crystals," *J Physical Soc Japan*, vol. 39, no. 4, pp. 1013–1021, Oct. 1975, doi: 10.1143/JPSJ.39.1013.

[20] M. Liu *et al.*, "Unveiling the charge storage mechanisms of perovskite fluoride KMnF3 in neutral aqueous electrolyte," *Energy Storage Mater*, vol. 63, p. 103004, Nov. 2023, doi: 10.1016/j.ensm.2023.103004.

[21] J. Zhao *et al.*, "Enhancing charge storage of O-doped perovskite fluorides via in-situ electrochemical oxidation for high-performance potassium-ion capacitors," *J Mater Sci Technol*, vol. 158, pp. 111–120, Sep. 2023, doi: 10.1016/j.jmst.2023.02.018.

[22] Z. Chen and L. Wen, "Controllable preparation of ultrafine KMnF3 perovskite by combining micro-channel reactor and microwave-ultrasonic assistance," *Chemical Engineering and Processing - Process Intensification*, vol. 183, p. 109220, Jan. 2023, doi: 10.1016/j.cep.2022.109220.